

The fate of Amazonian ecosystems over the coming century arising from changes in climate, atmospheric CO₂, and land use

KE ZHANG^{1,2,3}, ANDREA D. DE ALMEIDA CASTANHO^{4,5}, DAVID R. GALBRAITH⁶, SANAZ MOGHIM⁷, NAOMI M. LEVINE^{1,8}, RAFAEL L. BRAS^{7,9}, MICHAEL T. COE⁴, MARCOS H. COSTA¹⁰, YADVINDER MALHI¹¹, MARCOS LONGO¹, RYAN G. KNOX¹², SHAWNA MCKNIGHT⁷, JINGFENG WANG⁷ and PAUL R. MOORCROFT¹

¹Department of Organismic and Evolutionary Biology, Harvard University, Cambridge, MA, USA, ²Cooperative Institute for Mesoscale Meteorological Studies, University of Oklahoma, Norman, OK, USA, ³Hydrometeorology & Remote Sensing (HyDROS) Laboratory, School of Civil Engineering and Environmental Sciences, University of Oklahoma, Norman, OK, USA, ⁴The Woods Hole Research Center, Falmouth, MA, USA, ⁵Department of Agricultural Engineering, Federal University of Ceará, Fortaleza, Brazil, ⁶School of Geography, University of Leeds, Leeds, UK, ⁷School of Civil and Environmental Engineering, Georgia Institute of Technology, Atlanta, GA, USA, ⁸Department of Biological Sciences, University of Southern California, Los Angeles, CA, USA, ⁹School of Earth and Atmospheric Sciences, Georgia Institute of Technology, Atlanta, GA, USA, ¹⁰Department of Agricultural and Environmental Engineering, Federal University of Vicosa, Viçosa, Minas Gerais, Brazil, ¹¹Environmental Change Institute, School of Geography and the Environment, University of Oxford, Oxford, UK, ¹²Department of Civil and Environmental Engineering, Massachusetts Institute of Technology, Cambridge, MA, USA

Abstract

There is considerable interest in understanding the fate of the Amazon over the coming century in the face of climate change, rising atmospheric CO₂ levels, ongoing land transformation, and changing fire regimes within the region. In this analysis, we explore the fate of Amazonian ecosystems under the combined impact of these four environmental forcings using three terrestrial biosphere models (ED2, IBIS, and JULES) forced by three bias-corrected IPCC AR4 climate projections (PCM1, CCSM3, and HadCM3) under two land-use change scenarios. We assess the relative roles of climate change, CO₂ fertilization, land-use change, and fire in driving the projected changes in Amazonian biomass and forest extent. Our results indicate that the impacts of climate change are primarily determined by the direction and severity of projected changes in regional precipitation: under the driest climate projection, climate change alone is predicted to reduce Amazonian forest cover by an average of 14%. However, the models predict that CO₂ fertilization will enhance vegetation productivity and alleviate climate-induced increases in plant water stress, and, as a result, sustain high biomass forests, even under the driest climate scenario. Land-use change and climate-driven changes in fire frequency are predicted to cause additional aboveground biomass loss and reductions in forest extent. The relative impact of land use and fire dynamics compared to climate and CO₂ impacts varies considerably, depending on both the climate and land-use scenario, and on the terrestrial biosphere model used, highlighting the importance of improved quantitative understanding of all four factors – climate change, CO₂ fertilization effects, fire, and land use – to the fate of the Amazon over the coming century.

Keywords: Amazon, biomass, climate change, CO₂ fertilization, deforestation, fire, land use, terrestrial biosphere model, water stress

Received 12 June 2014; revised version received 24 November 2014 and accepted 11 December 2014

Introduction

Amazonian forest is a key component of the Earth's climate system and one of the largest terrestrial carbon reservoirs. Recent drought events in the region have been linked to increased rates of tree mortality (Phillips *et al.*, 2009; Lewis *et al.*, 2011) and increased fire

occurrence (Aragão *et al.*, 2007). Several GCM projections predict that, especially under the SRES A2 emission scenario, significant rainfall reductions will occur in eastern Amazonia over the coming century, with the steepest declines occurring during the dry season months (Malhi *et al.*, 2008) and that dry season length and intensity will increase (Malhi *et al.*, 2009; Costa & Pires, 2010), amplifying the occurrence of wet and dry months (Lintner *et al.*, 2012). A number of modeling studies using global dynamic vegetation models predict

Correspondence: Paul R. Moorcroft, tel. 617-496-6744, fax 617-496-8308, e-mail: paul_moorcroft@harvard.edu

that as much as 50% of the Amazon basin will be replaced by savanna and arid land vegetation by the end of the 21st century (Betts *et al.*, 2004; Cowling *et al.*, 2004; Cox *et al.*, 2004; Good *et al.*, 2011).

The resilience of Amazonian rainforests to changes in precipitation, temperature, and humidity over the basin still remains poorly understood: for example, satellite-derived observations indicate that Amazon forests green up during droughts due to increased availability of sunlight (Saleska *et al.*, 2007) that stimulates leaf flushing (Brando *et al.*, 2010). However, this has been disputed (REF), and forest inventory studies indicate increased tree mortality both during severe natural droughts (Phillips *et al.*, 2009) and under long-term experimental droughts (Nepstad *et al.*, 2007; Da Costa *et al.*, 2010).

Land-use change is also impacting on Amazonian ecosystems. Expansion of the cattle and soy industries in the Amazon basin during 1980s and 1990s increased rates of deforestation (Nepstad *et al.*, 2006), and past deforestation in the Brazilian Amazon has been estimated to be responsible for the release of approximately 0.2 GtC yr⁻¹ to the atmosphere (Houghton *et al.*, 2000). Deforestation rates have, however, decreased considerably since 2004 (INPE, 2014). Fire leakage from agricultural activities into areas of neighboring forest also occurs. Severe droughts in 1998 burned approximately 40 000 km² Amazon forest (Nepstad *et al.*, 2004), releasing approximately 0.4 GtC (De Mendonca *et al.*, 2004). In 2005, during the worst drought in 40 years, fires originating from fire leakage burnt an area of 2800 km² alone in the state of Acre, Brazil (Aragão *et al.*, 2007).

Another important consideration is the impact of human-induced increases in atmospheric CO₂ concentrations. Recent modeling studies predict a substantial CO₂ fertilization effect for Amazonian ecosystems (e.g., Rammig *et al.*, 2010; Cox *et al.*, 2013; Huntingford *et al.*, 2013). Findings of increasing biomass in studies of forest inventories in the tropics have been interpreted as indicating that CO₂ fertilization may be occurring (Baker *et al.*, 2004; Lewis *et al.*, 2009); however, there is currently limited direct evidence from large-scale experimental studies in tropical forests, such as free-air carbon dioxide enrichment (FACE) experiments, to support this conclusion.

The interactions and linkages between these environmental drivers are illustrated in Fig. 1. As the figure illustrates, climate change, land-use change, fire, and CO₂ fertilization are all potentially important drivers affecting the future fate of Amazonian ecosystems; however, their relative importance has not been assessed in previous analyses. In this study, we used three process-based terrestrial biosphere models to

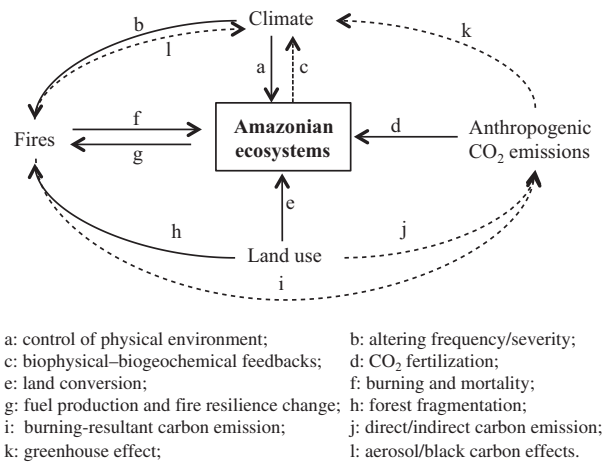


Fig. 1 Schematic diagram of the interactions between Amazonian ecosystems, climate, fire, land-use change, and anthropogenic CO₂ emissions. Solid arrows show the processes evaluated in this study [Based on the work by Cochrane (2003) and Golding & Betts (2008)].

investigate the impacts of these four driving forces on Amazonian ecosystems.

The objectives of this study are two-fold: (1) to assess the fate of Amazonian ecosystems in the 21st century, identifying the relative contributions of climate change, CO₂ rising, land-use change, and fire to future changes in Amazonian forest biomass and forest extent; and (2) to investigate the ecological responses caused by these environmental drivers and the accompanying differences in the model predictions. The uncoupled nature of the model simulations conducted here precludes incorporating ecosystem feedbacks on the climate system (arrow c, Fig. 1); however, our analysis incorporates predictions from three different biosphere models, which have been shown to be an important source of uncertainty in predicting climate-induced changes in Amazonian forest biomass (Rammig *et al.*, 2010).

Materials and methods

Terrestrial biosphere models

Three state-of-the-art terrestrial biosphere models were used in this study: the Ecosystem Demography Biosphere Model (ED2) (Moorcroft *et al.*, 2001; Medvigy *et al.*, 2009), the Integrated Biosphere Simulator (IBIS) (Foley *et al.*, 1996; Kucharik *et al.*, 2000), and the Joint UK Land Environment Simulator model (JULES) (Best *et al.*, 2011; Clark *et al.*, 2011).

ED2 is an individual-based terrestrial biosphere model providing a physically and biologically consistent framework suitable for both short-term (hourly to interannual) and long-term (interannual to multicentury) studies of terrestrial ecosystem dynamics. It simulates vegetation dynamics using

integrated submodels of plant growth and mortality, phenology, disturbance, biodiversity, hydrology, and soil biogeochemistry. In contrast to conventional 'ecosystem as big leaf' models that represent the plant canopy in a highly aggregated manner, ED2 uses a system of size- and age-structured partial differential equations (PDEs) to describe the behavior of a vertically stratified, spatially distributed collection of individual plants within each climatological grid cell (Moorcroft *et al.*, 2001; Medvigy *et al.*, 2009). The system of PDEs enables the model to: (1) track subgrid scale changes in the biophysical, ecological, and biogeochemical structure of the ecosystems; (2) incorporate the spatially localized competition between individuals; and (3) capture the impacts of subgrid scale disturbances on the structure and function of the ecosystem within each climatological grid cell. In this study, plant ecosystem diversity was represented using five tropical plant functional types (PFTs): (1) fast-growing, light-tolerant, pioneer tropical trees, (2) mid-successional tropical trees, (3) slow growing, shade-tolerant, late successional tropical trees, (4) C₃ grasses and forbs, and (5) C₄ grasses and forbs. Both density-independent (tree-fall and aging) and density-dependent (carbon starvation) mortalities are calculated for each individual. Fire is triggered when soil water content of the top 1-m depth falls below a threshold that is determined by soil texture; its intensity is a function of fuel load (i.e., total aboveground biomass).

IBIS is a comprehensive model of terrestrial biosphere processes that uses an integrated framework incorporating land surface biophysics, vegetation phenology, vegetation dynamics and competition, and terrestrial carbon and nutrient cycling (Foley *et al.*, 1996; Kucharik *et al.*, 2000). IBIS simulates land surface processes within each cell using two vegetation layers (woody and herbaceous plants) and six soil layers. IBIS simulates twelve PFTs that compete for light and water, of which four are relevant for this study: tropical broadleaf evergreen trees, tropical broadleaf drought-deciduous trees, evergreen shrubs, and warm grasses. Mortality is approximated using a constant woody biomass turnover rate. IBIS dynamically simulates fire and determines burnt area by soil dryness and fuel load (i.e., total carbon of litter pools).

JULES 2.1 is a process-based dynamic global vegetation model (DGVM) that simulates the fluxes of carbon, water, energy, and momentum between the land surface and the atmosphere (Best *et al.*, 2011; Clark *et al.*, 2011). It originated from the Met Office Surface Exchange Scheme (MOSES; Cox *et al.*, 1999; Essery & Clark, 2003). The model simulates five PFTs, of which four are relevant to the simulations for this study: broadleaf evergreen trees, shrubs, C₄ grasses, and C₃ grasses. The area covered by each PFT is determined by its net carbon gain, and the competition between PFTs is modeled using a Lotka-Volterra approach (Cox, 2001). Mortality is not explicitly represented in JULES, but is implicitly present as part of the background rate of woody biomass turnover. Fire is not simulated in the current implementation of JULES. All terrestrial biosphere models were forced by the same set of climate, land use, and CO₂ forcing data sets and had standardized soil physics. Further details on these are given in the following sections.

Climate data

The meteorological forcing variables used in the analysis consist of hourly scale estimates of atmospheric temperature, specific humidity, downward shortwave radiation, downward long-wave radiation, precipitation, wind speed, and air pressure. Shortwave radiation is further partitioned into direct and diffuse, visible and near-infrared components using the approach of Goudriaan (1977). It is well known that there are considerable biases in re-analysis meteorology and climate model predictions that lead to errors in the simulations of land processes (Berg *et al.*, 2003; Randall *et al.*, 2007; Zhang *et al.*, 2007). In addition, re-analysis data and climate model outputs generally have coarse spatiotemporal resolutions. To improve the accuracy of the terrestrial biosphere model simulations, a set of downscaling and bias-correction methods was therefore applied to the climate forcing data sets used in this study.

For the historical period (1700–2008), we used a downscaled, bias-corrected NCEP re-analysis database from 1970 to 2008 updated from Sheffield *et al.* (2006). The original data set has 1° spatial resolution and 3 hourly time resolution. For all meteorological variables except precipitation and shortwave radiation, the data were linearly interpolated to hourly resolution. The precipitation data were downscaled to hourly data to reflect the point-scale statistical characteristics of local rain gauge measurements using the approach of Eltahir & Bras (1993) and Lammering & Dwyer (2000). Downward shortwave radiation was interpolated to hourly resolution using the solar zenith angle as a function of solar declination, latitude, and hour angle of each pixel (Knox, 2012). More details on the downscaling and bias-correction methods can be found in Knox (2012) and Moghim S, Mcknight S, Zhang K, Knox RG, Bras RL, Moorcroft PR (submitted). Hereafter, NCEP denotes the 1 hourly, 1° bias-corrected NCEP data set except as otherwise noted.

The projections of future climate (2009–2100) were obtained from simulations of three general circulation models (GCMs) under the SRES A2 scenario for which subdaily outputs were available, including the parallel climate model (PCM1), the community climate system model (CCSM3), and the Hadley Centre coupled model (HadCM3). While the SRES A2 scenario was developed as a worst-case scenario, in which CO₂ emissions increase fourfold over this century (Nakicenovic *et al.*, 2000), the growth in CO₂ emissions in the last decade has been close to the A2 scenario and in some years even exceeded it (Le Quere *et al.*, 2009).

The outputs of the three GCMs were regridded to 1° and 1-h resolution and corrected for biases. Biases in precipitation and temperature fields were corrected by applying the equidistant cumulative distribution function (EDCDF) matching method (Li *et al.*, 2010; Moghim S, Mcknight S, Zhang K, Knox RG, Bras RL, Moorcroft PR, submitted). Specific humidity and downward long-wave radiation were then correspondingly adjusted using the bias-corrected temperature data Moghim S, Mcknight S, Zhang K, Knox RG, Bras RL, Moorcroft PR, (submitted). Hereafter, unless noted otherwise, PCM, CCSM3, and HadCM3 refer to the hourly, 1° bias-corrected versions of the respective data set.

There are considerable differences between the projected climatologies by the three GCMs. All three predict significant ($P < 0.01$), regionwide warming trends over the 21st century; however, the magnitudes of warming trends differ: HadCM3 has the strongest warming trend over the region ($0.45\text{ }^{\circ}\text{C de}^{-1}$), followed by CCSM3 ($0.38\text{ }^{\circ}\text{C de}^{-1}$) and PCM ($0.13\text{ }^{\circ}\text{C de}^{-1}$) (Table 1). Their projected changes in precipitation also differ: HadCM3 projection indicates that approximately half (53%) of the region, mainly the eastern and southeastern Amazon, will suffer significant rainfall reductions during the 21st century, while PCM and CCSM3 predict that significant portions of the basin (47% and 62% of the region, respectively), located mainly in southern and western portions of the basin, will experience significant increases in precipitation. Further details regarding comparison can be found in Appendix S1.

Comparison of these predictions against the 19 GCM projections examined by Malhi *et al.* (2009) indicates that they span the range of climate predictions for the Amazon region: the PCM projection presents a slightly warmer but wetter future climate, while the HadCM3 projection represents an extremely hot and dry scenario, and the CCSM3 projection falls in-between (Table 1). The above three climate projections enable us to evaluate the response and sensitivity of Amazonian ecosystems under the range of future climate change scenarios predicted for this region.

Land-use data

The historical land-use transition rates used in the study were calculated from the global land-use data set (GLU) that incorporates the SAGE-HYDE 3.3.1 data set and provides global land-use transitions on a 1° grid from 1700 to 1999 (Hurt *et al.*, 2006). Following Albani *et al.* (2006), three land-use states: primary vegetation, secondary vegetation, and agricultural land were represented, and the GLU transition rates were converted into corresponding transition rates among these three land-use states. For future land use (2009–2050), two Amazon land-use scenarios from Soares-Filho *et al.* (2006) were used: the first is a ‘business-as-usual’ scenario (BAU) that assumes continuation of the deforestation rates estimated during the 2001–2002 period, paving highways as scheduled, low forest reserves on private land, and no new protected areas; the second is a ‘governance’ scenario (GOV), which assumes that Brazilian environmental legislation is maintained across the Amazon basin (Soares-Filho *et al.*, 2006). The

BAU and GOV data sets were harmonized with the GLU data set and extended to 2100 to produce consistent land-use transition data for the entire period (1700–2100) (Appendix S2). Primary vegetation in the Amazon under the GOV and BAU scenarios declines from 61% in 2008 to 51% and 33% in 2100, respectively (Fig. S2). The spatial patterns of future deforestation are closely associated with the spatial distribution of future highway network (Soares-Filho *et al.*, 2006).

Soils and atmospheric CO₂ data

Atmospheric CO₂ concentrations for the simulation period were generated by fitting an exponential function to the ice-core CO₂ data (Epica Community Members, 2004) for the 1700–1859 period, and then merging this trajectory with the observed CO₂ concentrations for the rest of the historical period, and with the SRES A2 CO₂ concentrations (Nakicenovic *et al.*, 2000) for the future period. The Soil physics was standardized for all models: identical pedotransfer functions from Clapp & Hornberger (1978) were used for all models, with the parameters of the functions depending on the sand and clay fractions of soils. The sand and clay fractions were specified from the Quesada *et al.* (2010) data set where available and elsewhere from the IGBP-DIS global soil data (<http://daac.ornl.gov/SOILS/guides/igbp-surfaces.html>). Each soil type in the Quesada data was first assigned its mean sand and clay fraction values, and the derived 1 km sand and clay fraction data were then aggregated to 1-degree resolution. Due to insufficient soil depth data, we assumed a homogeneous soil depth of 10 m across the region.

Experimental design and statistical analysis

Due to the computationally intensive nature of the simulations, a full factorial analysis quantitating the magnitude between direct effects and all possible interactions was not feasible. Instead, the four factors [climate change (M), CO₂ fertilization (C), fires (F), and deforestation caused by land-use change (D)] were varied in a stepwise hierarchical manner (Table 2). Under this scheme, the effect of climate (M) is the direct effect of climate on the ecosystem; the effect of CO₂ (C) is the combined effect of its direct effects on the ecosystem and its interaction with M ; the effect of fires (F) is the combined effect of its direct effect on the ecosystem and its interactions associated with M and C ; and the effect of land use (D) is the combined effect of its direct effect and its interactions with

Table 1 Summary of the environmental trends over Amazonia in the bias-corrected data-sets for the historical period (1970–2008) and the future prediction period (2009–2100)

Time Period	Source of Meteorology	Tair ($^{\circ}\text{C de}^{-1}$)	VPD (Pa de^{-1})	Precipitation ($\text{mm yr}^{-1}\text{ de}^{-1}$)	CO ₂ (ppm de^{-1})	MCWD (mm de^{-1})
1970–2008 (historical)	NCEP	0.23***	30.03***	2.94	13.95***	–9.81
2009–2100 (prediction)	PCM	0.13***	–1.76	15.49***	45.24***	14.15**
	CCSM3	0.38***	29.52***	24.45***	45.24***	0.92
	HadCM3	0.45***	68.86***	–21.05**	45.24***	66.53**

** $P < 0.05$; *** $P < 0.01$.

Table 2 Summary of the factorial model simulations conducted in this study

Simulation*	Description	Meteorology Forcing†	Models
Control	Simulation with 2000–2008 climate variability, no further land-use change and no further CO ₂ emissions	NCEP	All
M	Predicted 2009–2100 climate variability from GCMs, no further CO ₂ emissions, and no fire activity	PCM, CCSM3, HadCM3	All
MC	Predicted 2009–2100 climate variability from GCMs in conjunction with the IPCC AR4 SRES A2 CO ₂ emissions, but no wildfire activity	PCM, CCSM3, HadCM3	All
MF	Predicted 2009–2100 climate variability from GCMs with wildfire activity on, and no further CO ₂ emissions	PCM, CCSM3, HadCM3	ED2 and IBIS
MCD _G	Predicted 2009–2100 climate variability from GCMs, IPCC AR4 SRES A2 CO ₂ emissions, governance land-use scenario, and no wildfire activity	PCM, CCSM3, HadCM3	JULES
MCFD _G	Predicted 2009–2100 climate variability from GCMs, IPCC AR4 SRES A2 CO ₂ emissions, and governance land-use scenario with wildfire activity	PCM, CCSM3, HadCM3	ED2 and IBIS
MCD _B	Predicted 2009–2100 climate variability from GCMs in conjunction, IPCC AR4 SRES A2 CO ₂ emissions, BAU land-use scenario, and no wildfire activity	PCM, CCSM3, HadCM3	JULES
MCFD _B	Predicted 2009–2100 climate variability from GCMs, IPCC AR4 SRES A2 CO ₂ emissions, and BAU land-use scenario with wildfire activity	PCM, CCSM3, HadCM3	ED2 and IBIS

*The factors are as follows: *M*, climate; *C*, CO₂; *F*, fire; *D_G*, governance land use; *D_B*, business-as-usual land use.

†Bias correction was performed on all the meteorological forcing data sets.

M, *C*, and *F*. A control simulation with 2000–2008 climate variability, but with no further land-use change, and no further increase in atmospheric CO₂ concentrations was also conducted for each model. Table 2 summarizes the suite of simulations conducted in this study.

The simulations to establish the present-day state of Amazonian ecosystems were conducted for each terrestrial biosphere model using following the procedure: each model was run to its pre-industrial equilibrium state from near-bare ground using recycled historical climate forcing and constant pre-industrial atmospheric CO₂ concentration (278 ppm). The models were then run from their pre-industrial equilibrium in 1715 through 2008 driven by cycled historical climate forcing in conjunction with rising atmospheric CO₂ concentrations and historical land-use data.

The statistical significance of temporal trends of all variables either on the grid cell basis or at the regional level was tested by the Mann–Kendall nonparametric test. All statistical hypothesis tests were tested at a significance level of 0.1, if applicable, and further delineated at 90%, 95%, and 99% confidence intervals denoted by *, **, and ***, respectively.

Quantitation of climatic water stress

Consistent with previous analyses (e.g., Malhi *et al.*, 2009; Good *et al.*, 2011), we used maximum climatic water deficit (MCWD) as a metric to quantitate changes in water-stress regimes. MCWD is defined here as the lowest (i.e., most negative) value of the monthly climatic water deficit (CWD_{*n*}) during a year, that is:

$$\text{MCWD} = \min(\text{CWD}_1, \dots, \text{CWD}_{12}), \quad (1)$$

where the monthly climatic water deficit values CWD_{*n*} (*n* = 1...12) are calculated as the integrated difference between monthly precipitation and potential evapotranspiration during the prior months of the year, that is:

$$\text{CWD}_n = \sum_{i=0}^{11} (P_{n-i} - \text{PET}_{n-i}), \quad (2)$$

where *P_i* and *PET_i* are, respectively, the precipitation and potential evapotranspiration in month *i*. This definition is similar to that of Malhi *et al.* (2009), but rather than assuming a constant water demand of 100 mm month⁻¹ evapotranspiration rate as in Malhi *et al.* (2009) and Good *et al.* (2011), monthly potential evapotranspiration (PET) was calculated directly using the Penman equation (rewritten in metric units by Shuttleworth (1993)), thereby incorporating the impacts of the changing atmospheric conditions on climatic water demand.

Results

We first assessed the ability of the three terrestrial biosphere models to capture the extant spatial patterns of regional aboveground live biomass (AGB) and percent tree cover by comparing model predictions of these quantities against two satellite-based AGB from Saatchi *et al.* (2011) and Baccini *et al.* (2012) and satellite-derived estimates of percent tree cover (Dimiceli *et al.*, 2011). Overall, the comparisons show that the biosphere models are able to reasonably capture the present-day spatial variability of Amazonian AGB and tree

cover that are observed by satellites. Further details of regarding strengths and limitations of each model's predictions can be found in the section below and Appendix S3.

Predicted and observed relationships between aboveground biomass and water stress across the basin

We examined the relationship between AGB and the MCWD metric measuring the intensity of water stress (Fig. 2). There are some notable differences in the range of AGB estimates between the two remote sensing data sets, particularly at regions with large negative MCWDs (Fig. 2), highlighting the uncertainty in regional-scale estimates of AGB. In low to intermediate water-stress areas (+1800 to 0 mm MCWD), the AGB values predicted by ED2 and IBIS generally agree well with the remote sensing estimates of AGB, while JULES predicts AGB values that are systematically higher than the other two models and the remote sensing products (Fig. 2). In the driest areas (−600 to −1200 mm MCWD), ED2 and IBIS tend to underestimate AGB while JULES shows better agreement with the remote sensing products in these areas (Fig. 2). This is likely due in part to an overestimate of fire impacts in these regions by ED2 and IBIS, while fire is not simulated in

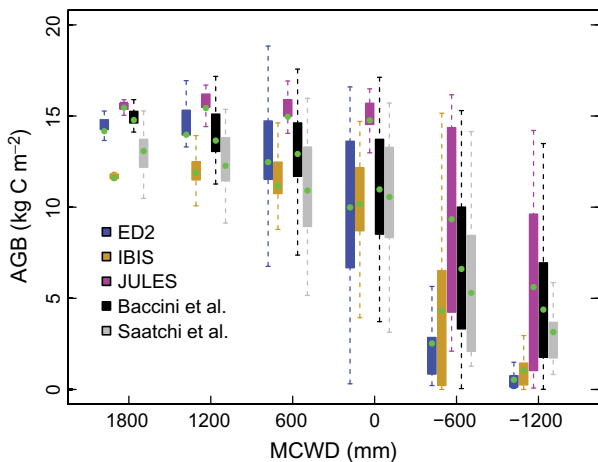


Fig. 2 Predicted and observed patterns of aboveground biomass (AGB) as a function of maximum climatological water deficit (MCWD) across the Amazon gridded at 1-degree resolution. The predicted AGB values are the present-day estimates from the three biosphere models while the two observed values are corresponding satellite-derived estimates of Baccini *et al.* (2012) and Saatchi *et al.* (2011) gridded at the same resolution as the simulations. The MCWD values for each climatological grid cells were calculated from the bias-corrected NCEP reanalysis for the period 2000–2008. Each box plot shows the distribution of AGB within each MCWD class, while the green points denote the mean values.

JULES. Both the remote sensing measurements and model predictions of AGB show strong and significant associations with MCWD (Table S1). AGB generally decreases as MCWD becomes more negative (Fig. 2), indicative of the role that water stress plays in governing the spatial variation of aboveground biomass across the region.

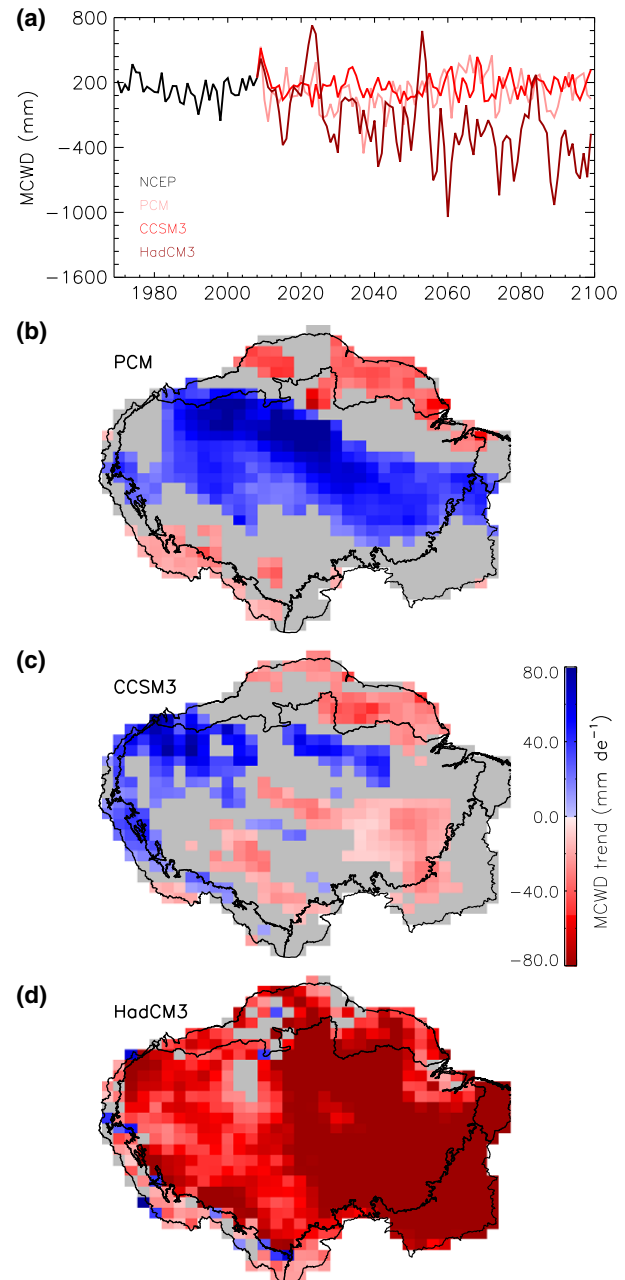


Fig. 3 Time series of regional mean (a) MCWD for the historical (1970–2008) and prediction (2009–2100) periods, and spatial patterns of the temporal trends in MCWD from 2009 to 2100 under (b) the PCM, (c) CCSM3, and (d) HadCM3 climate projections.

Predicted changes in water stress over the coming century

All three climate projections show changes in the region's water-stress regimes in the 21st century (Fig. 3). The PCM climate model predicts that the Amazon as a whole will experience an alleviation of water stress (basinwide average MCWD increases by 14.15 mm de^{-1} ; $P < 0.1$) in the 21st century (Fig. 3a), with significant reductions in water stress occurring in about 41% of the region (Fig. 3b). The CCSM3 climate model predicts no significant change in basin average MCWD (Fig. 3a), but significant upward trends (i.e., alleviation of drought severity) in the western Amazon and significant downward trends (i.e., aggravation of drought severity) in the southeastern and northern Amazon (Fig. 3c). In contrast, the HadCM3 climate model projects substantial increases in water stress across Amazonia, as implied by the strong negative trend in MCWD ($-66.53 \text{ mm de}^{-1}$; $P < 0.01$) (Fig. 3a), and the spatial extent of changes in water stress (Fig. 3d). These GCM projections represent a wide range of climate change trajectories, ranging from relatively benign shifts in region's climatology in the 21st century projected by PCM to a severe hot and dry climatology projected by HadCM3.

Factorial contribution of drivers of ecosystem change

The relative contributions of the four drivers to changes in ecosystem aboveground biomass (ΔAGB) predicted by the three models are summarized in Fig. 4. The effects of fire could only be evaluated using ED2 and IBIS because, as noted earlier (see *Materials and Methods* section), the current implementation of JULES doesn't simulate fire dynamics.

All three biosphere models predict a strong positive impact of CO_2 on AGB (green bars in Fig. 4a–c); however, the magnitude of this CO_2 fertilization effect varies between the models: ED2 exhibits the strongest CO_2 effect ($0.147\text{--}0.149 \text{ GtC ppm}^{-1}$), followed by IBIS ($0.113\text{--}0.119 \text{ GtC ppm}^{-1}$) and JULES ($0.03\text{--}0.05 \text{ GtC ppm}^{-1}$). The effect of climate change (red bars in Fig. 4) is much more variable across the models. Both ED2 and IBIS predict positive impacts of climate on AGB under the PCM and CCSM3 climate trajectories, which have mild warming trends, and predict no change or a relaxation in levels of water stress (Fig. 4a and b), while JULES predicts uniformly negative effects of the future climate trajectories on AGB (Fig. 4c). Both ED2 and JULES predict that the HadCM3 climate trajectory, the hottest and driest one of the three climate scenarios, causes strong reductions in regional AGB (Fig. 4a and c), while IBIS predicts that the HadCM3

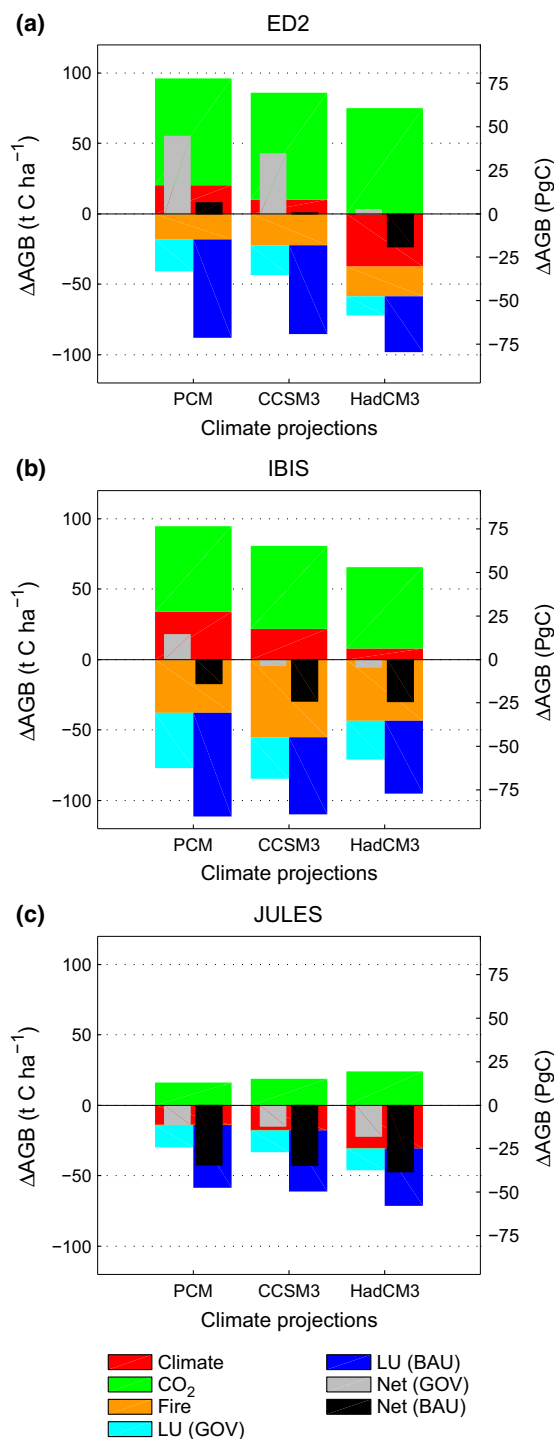


Fig. 4 The contributions of different environmental forcings (climate, CO_2 , fire and land use) to the changes in Amazonian aboveground live biomass from 2009 to 2100 predicted by the three biosphere models (ED2, IBIS, and JULES) under the three GCM climate projections (PCM, CCSM3, and HadCM3). The combined net effects of all forcings (i.e. climate + CO_2 + fire + land use) under the two land-use scenarios (BAU and GOV) are also shown.

climatology leads to a slightly positive contribution to regional AGB (Fig. 4b). In both ED2 and IBIS, fires decrease AGB under all climate trajectories, but the magnitude of the losses is considerably larger in IBIS compared to ED2 (orange bars in Fig. 4 panels a and b).

Land-use change imposes negative effects on AGB across all models and climate trajectories, the extent varying greatly between the land-use scenarios (see Fig. 4a–c). The impacts of land-use change on AGB are diminished under the severe HadCM3 climatology (see changes in the size of light and dark blue bars under different climate trajectories in Fig. 6.), indicating an interactive effect of land use and climate. With the exception of the JULES' prediction under the HadCM3 climate trajectory, the models predict that under the BAU land-use scenario, the impacts of land use on AGB outweigh the impact of climate change (compare the red and dark blue bars in Fig. 4). However, under the GOV land-use scenario, the impacts of climate change on AGB are of comparable magnitude and, in some cases, exceed the effects of land-use change (compare the red and light blue bars in Fig. 4).

The combined net effect of all the environmental factors (see gray and black bars in Fig. 4) differs among the models. In JULES, the net effect results in AGB loss

under the three climate trajectories in conjunction with either of the two land-use scenarios (Fig. 4c), while IBIS predicts net losses in AGB for all combinations except for the most favorable combination (i.e., the PCM climatology plus the GOV land use) (Fig. 4b). In contrast, ED2 predicts net gains in AGB for all combinations except for the severest combination (i.e., the HadCM3 climatology plus the BAU land use) (Fig. 4a).

The climate change trajectories have different impacts on spatial patterns of AGB across the three biosphere models (Fig. 5). In ED2, the PCM and CCSM3 climate trajectories cause AGB to increase (+0.5 to +8.0 kgC m⁻²) over most of the Amazon basin by the end of century, accompanied by decreases in AGB in a few areas in the south (PCM), or south and east (CCSM3) of the basin. Under the HadCM3, however, regionwide losses in AGB (–1.0 to –15.0 kgC m⁻²) occur (Fig. 5). In IBIS, the PCM climate trajectory leads to widespread increases in AGB, especially in the southern and southeastern cerrado regions (Fig. 5), with the increases ranging from +1.0 kgC m⁻² in the central Amazon to +15.0 kgC m⁻² in the southeastern region. Under the CCSM3 climate trajectory, IBIS predicts widespread increases in AGB in the southern and southeastern areas, but decreases in AGB in the western Amazon.

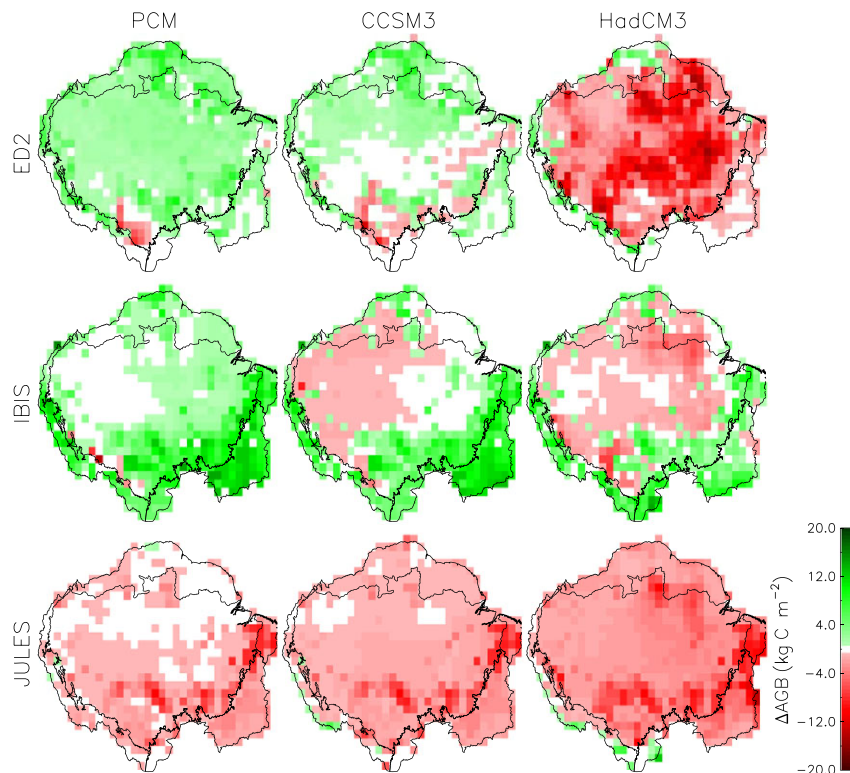


Fig. 5 Maps showing the contribution of climate change to the changes in Amazonian aboveground live biomass (AGB) from 2009 to 2100 predicted by the three biosphere models (ED2, IBIS, and JULES) under the PCM, CCSM3, and HadCM3 climate projections.

Under the HadCM3 climate trajectory, AGB decreases (-0.5 to -9.0 kgC m^{-2}) over most of the basin (Fig. 5). Unlike ED2 and IBIS, JULES predicts a negative impact on AGB under all three climate trajectories, ranging from -0.5 to -10.0 kgC m^{-2} under the PCM trajectory to -1.0 to -14.0 kgC m^{-2} under the HadCM3 trajectory (Fig. 5).

Compared to the effects of climate, the effects of CO_2 , fire, and land use on AGB show more consistency

across the models. Although the magnitude and spatial extent of the CO_2 fertilization effects vary in all models, elevated CO_2 leads to AGB increases across the Amazon basin with smaller increases occurring in the drier, low biomass cerrado regions and in the Andes Mountains (Fig. 6a). Consistent with the results seen in Figure 4a–c, the CO_2 fertilization effect is larger in ED2 and IBIS than in JULES (Fig. 6a). The effects of elevated CO_2 show little spatial variability in IBIS and JULES,

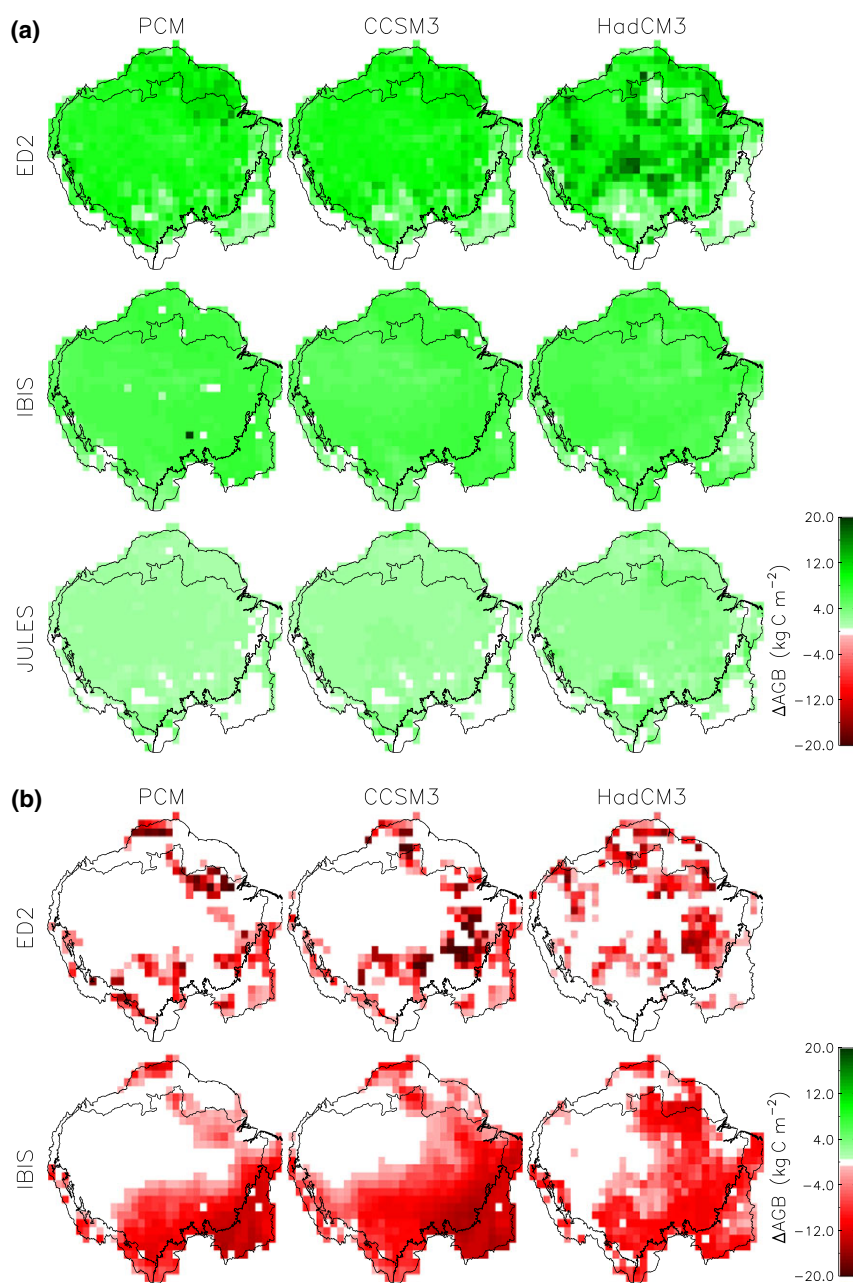


Fig. 6 Maps showing the contributions of (a) CO_2 fertilization, and (b) fire, to the changes in Amazonian aboveground live biomass from 2009 to 2100 predicted by the three biosphere models (ED2, IBIS, and JULES) under the PCM, CCSM3, and HadCM3 climate projections.

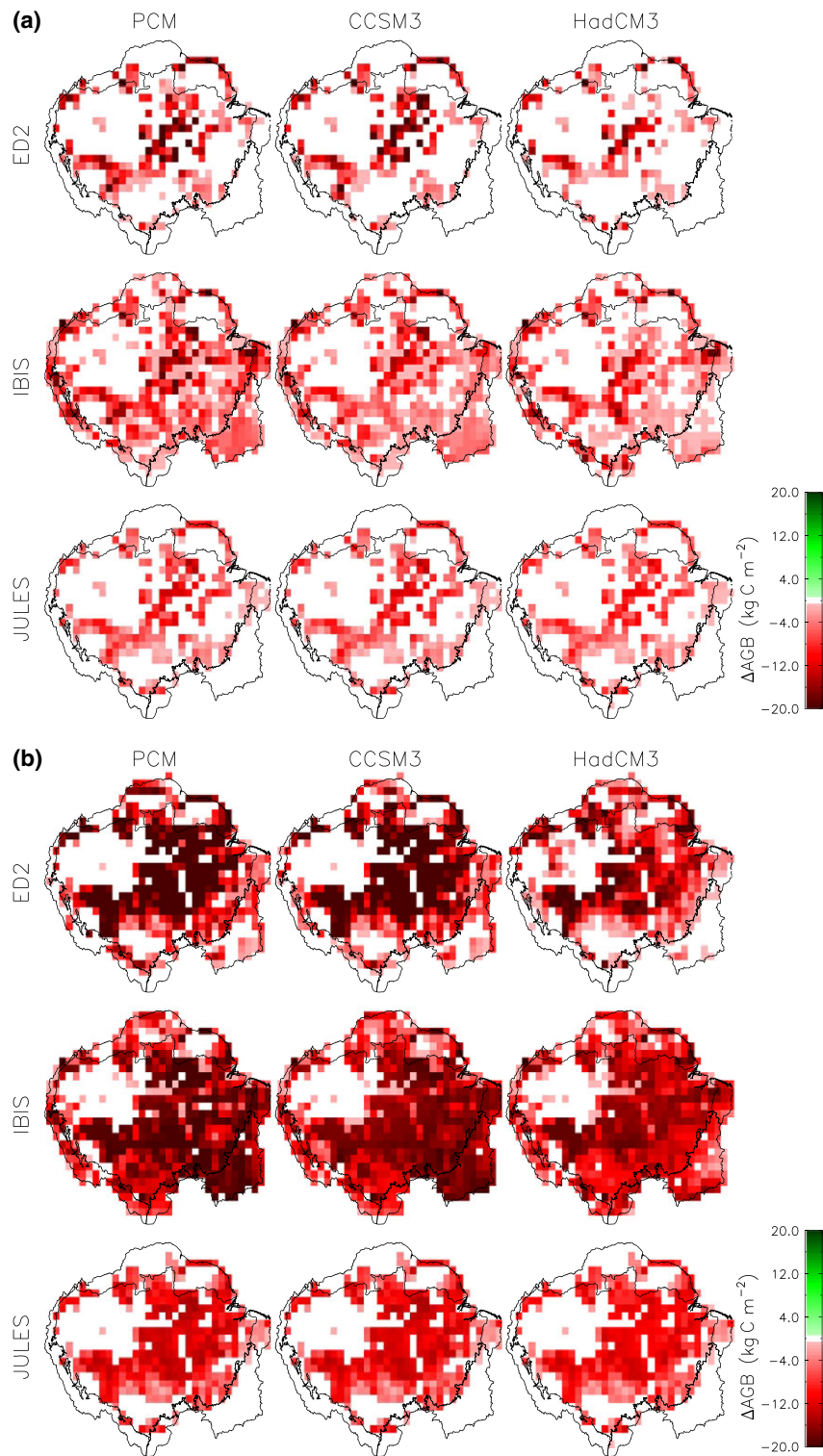


Fig. 7 Maps showing the contributions of (a) GOV land use, and (b) BAU land use, to the changes in Amazonian aboveground live biomass (AGB) from 2009 to 2100 predicted by the three biosphere models (ED2, IBIS, and JULES) under the PCM, CCSM3, and HadCM3 climate projections.

ranging from 0.16 to 0.23 $\text{kgC m}^{-2} \text{de}^{-1}$ and from 0.09 to 0.13 $\text{kgC m}^{-2} \text{de}^{-1}$, respectively, but a slightly larger spatial variability in ED2 (0.34–0.5 $\text{kgC m}^{-2} \text{de}^{-1}$) (Fig. 6a).

Fires have a significant negative impact on AGB in both ED2 and IBIS; however, the magnitude and spatial distribution of its impact varies considerably between the two models (Fig. 6b): In ED2, fire caused biomass loss occurs primarily at the edge of the current forest areas and adjacent areas, while the effect in IBIS across most of the eastern, central, southern Amazon (Fig. 6b).

As expected, land use has negative impacts on AGB across all models, with a larger and more spatially extensive, impact under the BAU compared to the GOV land-use scenario, particularly in the eastern and southern Amazon (Fig. 7). Overall, the GOV and BAU scenarios are projected to reduce Amazonian AGB by 11.0–31.8 GtC and 35.0–59.7 GtC, respectively (blue bars in Fig. 4). The magnitude of their effects on AGB differs across the climate trajectories due to the interactions between climate change and land-use change (Fig. 7). The magnitude of the land-use impacts on AGB

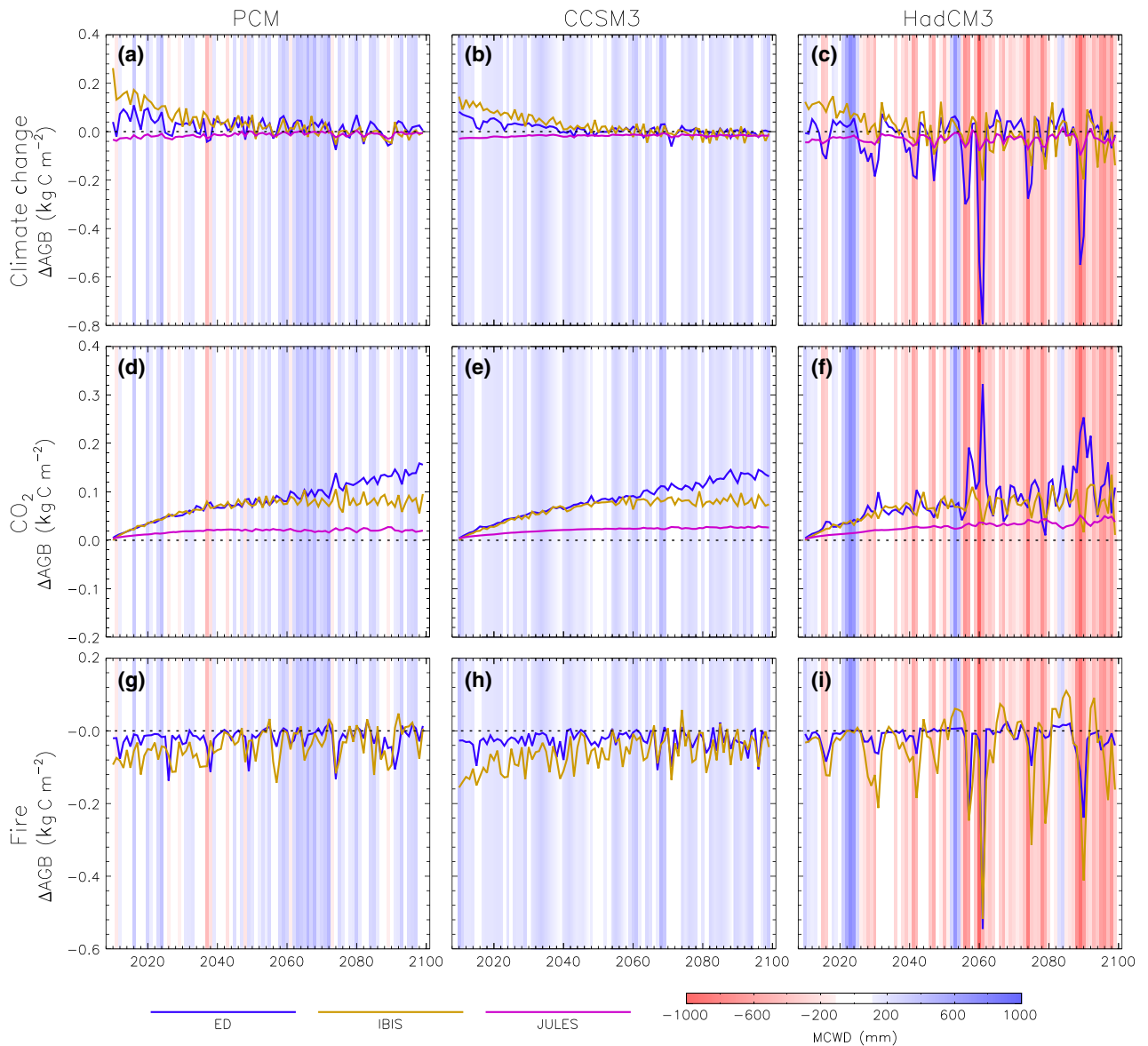


Fig. 8 Temporal variation in the contributions of climate change (panels a–c), atmospheric CO_2 (panels d–f) and fire (panels g–i), to the changes in aboveground biomass (ΔAGB) from 2009 to 2100 derived from the three biosphere models under the PCM, CCSM3, and HadCM3 projected climatologies. The blue shading and red shading, respectively, indicate periods of climatic water surplus and deficit as estimated by changes in the average MCWD across the simulation region.

also differs across models with generally larger magnitude impacts in IBIS compared to ED2 and JULES (Fig. 7).

Trends and interannual variability in aboveground biomass change

In all models, the impacts of climate change on AGB are positively correlated with annual MCWD ($r = 0.34$ – 0.72 ; $P < 0.001$) (Fig. 8a–c), indicating that all models are responsive to interannual variability in water-stress levels. However, the climate effect shows much larger interannual variation in ED2 and IBIS than in JULES (Fig. 8a–c). In ED2 and IBIS, the effect of climate fluctuates between the negative and positive phases, while the climate effect in JULES on regional AGB is relatively small and consistently negative. ED2 exhibits the highest sensitivity to episodic drought events, indicated by the largest climate-caused reductions in AGB in the driest years (e.g., years 2060, 2074, and 2089 in the HadCM3 climatology), followed by IBIS and JULES (Fig. 8a–c). Although JULES predicts the lowest AGB reductions during the driest years, the constantly negative, small effect of climate in JULES leads to cumulatively large reductions in AGB under all three future climate trajectories (Fig. 5).

CO₂ fertilization causes AGB to increase over time in all models due to the increasing CO₂ concentrations with time (Fig. 8d–f), but consistent with the patterns seen in Figs 4 and 6a, and the magnitude of the effect varies considerably between the three models, being strongest in ED2 ($0.83 \text{ kgC m}^{-2} \text{ de}^{-1}$), intermediate in IBIS ($0.65 \text{ kgC m}^{-2} \text{ de}^{-1}$), and lowest in JULES ($0.22 \text{ kgC m}^{-2} \text{ de}^{-1}$). In addition, the CO₂ fertilization effect in IBIS and JULES levels off after ~2060 when atmospheric CO₂ concentrations reach approximately 562 ppm, which does not occur in ED2 (Fig. 8d–f). There is little interannual variation in the CO₂ effect in most years, but during extremely dry years (e.g., years of 2060, 2074, and 2089 in the HadCM3 climate trajectory), CO₂ has a strong compensating effect on the negative impacts of climate (compare Figs. 8c, f).

The effect of fire on AGB exhibits larger interannual variability than the effects of CO₂, and its impact becomes more evident during the driest years (Fig. 8g–i). The temporal patterns of fire effect on AGB are similar in ED2 and IBIS ($r = 0.70$; $P < 0.001$), although the magnitude of interannual variability is generally larger in IBIS than in ED2.

Although all models predict that future AGB will respond to changes in future water-stress regimes (Fig. 8a), the sensitivity of AGB changes to water-stress changes differs among the models. ED2 has the highest sensitivity to the extreme drought events, followed by

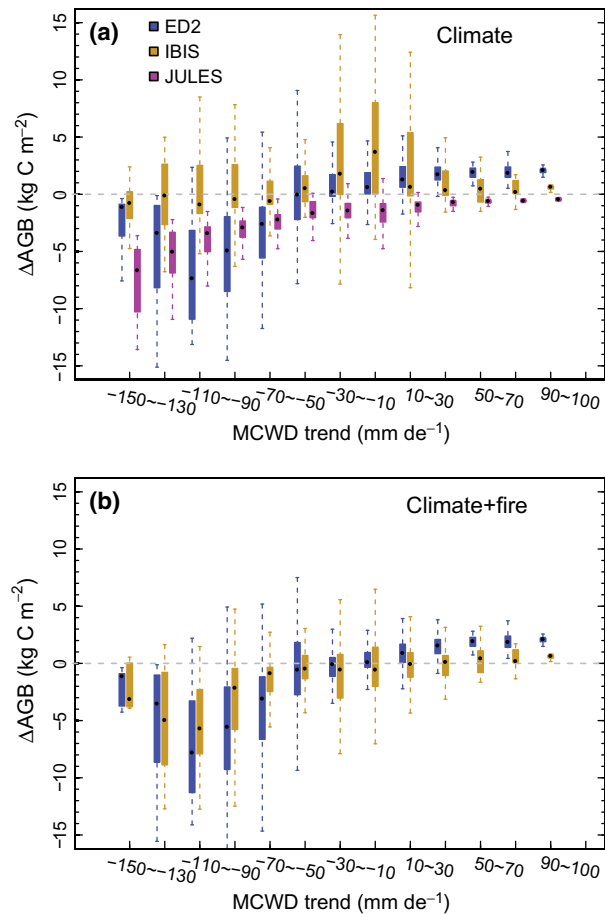


Fig. 9 The relationship between the decadal-scale MCWD trends from 2009 to 2100 within the climatological grid cells of the simulation region and corresponding aboveground biomass change (ΔAGB) over the period caused by (a) climate change, and (b) the sum of climate change and fire. Each box plot shows the distribution of predicted ΔAGB values for each MCWD class. Results from the three climate simulations and three climate + fire simulations (the *M* and *MF* simulations respectively, see Table 2) were used to calculate these relationships.

IBIS, while JULES has the lowest sensitivity to these events (Fig. 8a–c). However, IBIS has generally higher growth/recovery rates in AGB under favorable conditions than ED2 and JULES (Fig. 8a–c). As a result, the accumulated AGB loss caused by cumulative water stress is less evident in IBIS compared to ED2 and JULES (Fig. 9a). Although JULES exhibits the lowest AGB reductions during the driest years (Fig. 8a–c), the constant negative effect imposed by climate in JULES appears across almost all Amazonian grid cells, even these areas with relaxed water stress (Fig. 9a). In contrast, ED2 and IBIS predict that climate change will exert accumulated positive impacts on AGB in areas that experience reductions in water stress (i.e., positive trends in MCWD) (Fig. 9a). Once the effects of climate

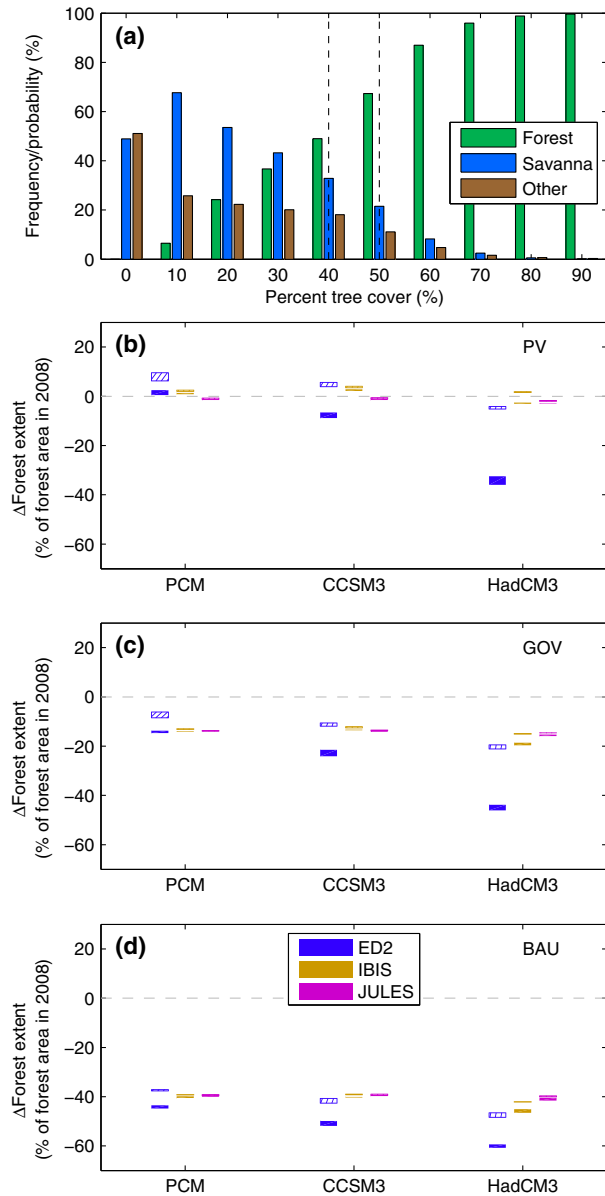


Fig. 10 (a) Histogram of percent tree cover by vegetation types across Amazonia and changes in Amazonian forest extent from 2009 to 2100 predicted by the ED2, IBIS, and JULES terrestrial biosphere models under the (b) potential vegetation (PV, i.e. no deforestation), (c) GOV land-use, and (d) BAU land-use scenarios given the changes in climate projected by the PCM, CCSM3 and HadCM3 climate scenarios. The percent tree cover and land cover data shown in panel (a) are from the MODIS collection 5 MOD44B and MCD12Q1 products respectively. The dashed vertical lines in this panel denote the range of thresholds used to distinguish between forest and nonforest types. The heights of boxes in panels (b)–(d) denote the range of predicted changes in Amazonian forest extent for the range of thresholds used to distinguish between forest and nonforest types. The hatched and solid boxes respectively denote the predictions with and without increasing atmospheric CO₂ levels.

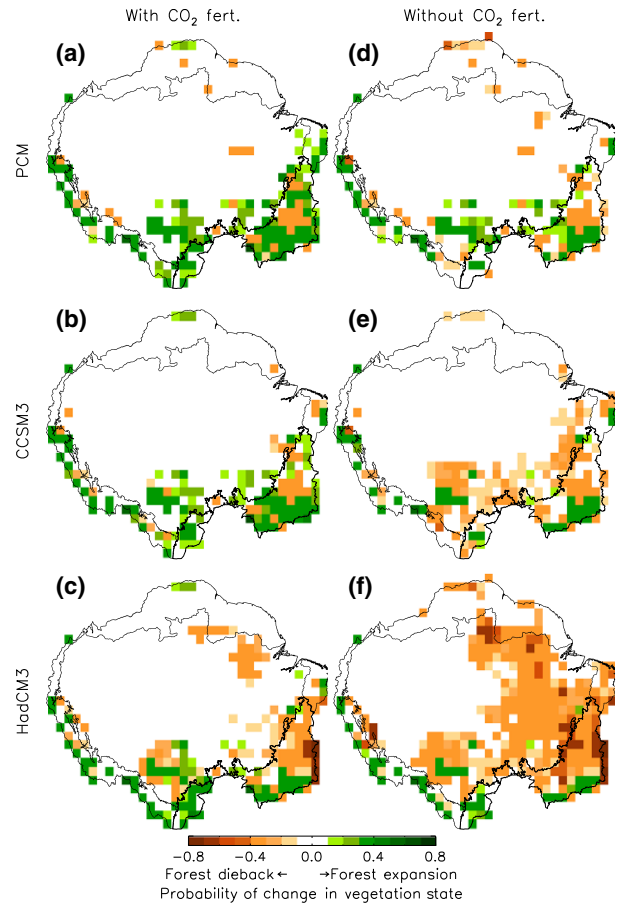


Fig. 11 The predicted probabilities of change in the potential vegetation (PV) state from 2009 to 2100 across Amazonia under (a) the PCM, (b) CCSM3, and (c) HadCM3 climate change trajectories, and (d–e) the predicted probability of change after removing the effects of CO₂ fertilization. The probability values reflect the probability of change for each grid cell averaged across the three terrestrial biosphere models and the range of thresholds used to distinguish between forest and nonforest types shown in Fig. 10a.

and fire are combined, ED2 and IBIS interestingly exhibit similar sensitivities to changes in water stress (Fig. 9b).

Changes in forest extent

To quantitate the changes in forest extent predicted by the three models across the Amazon, we calculated the estimated changes in percent tree cover, a common metric used to distinguish and infer forest and nonforest vegetation types. The percent tree cover was calculated as the fully projected tree foliage cover by following Kucharik *et al.* (2000): $f_{\text{treecover}} = 1 - \exp(-0.5 \times LAI_{\text{tree}})$, where 0.5 is an empirical canopy extinction coefficient, LAI_{tree} is the total leaf

area index of all tree PFTs. Following Hirota *et al.* (2011), we derived a threshold to distinguish between forest and nonforest states from the histograms of satellite-derived percent tree cover (MODIS collection 5 MOD44B product) stratified by the vegetation types (MODIS collection 5 MCD12Q1 product). There is a threshold of percent tree cover between 40% and 50% that distinguishes between forested and nonforested grid cells (Fig. 10a). To consider the sensitivity of the predictions to the threshold used to distinguish the vegetation types, the percent tree cover threshold that was used to convert the modeled percent tree cover value of each grid cell to a corresponding vegetation state (forest vs. nonforest) was varied between 40% and 50%.

In the absence of land-use change, the projected changes in forest extent from 2009 to 2100 vary between -5% and +10% (Fig. 10b). Under more favorable PCM and CCSM3 climate trajectories with rising CO₂, ED2 and IBIS predict an expansion of the Amazonian forests by 2%–10% while JULES predicts a reduction of forest area by 0.6%–1.3% (Fig. 10b). If the CO₂ fertilization effect is excluded, the projected changes in forest extent vary between -36% and +2.9% (Fig. 10b). The areas that likely experience changes in vegetation type are located in the savanna zones, the border between forest and savanna, and the Andes mountain range under the PCM and CCSM3 trajectories (Fig. 11a and b). Most of these areas are projected to convert from savanna into forest. Under the CCSM3 climate trajectory, the savanna areas adjacent to the south and southeastern borders of the Amazon forest, and in the central Andes mountain range are predicted to convert into forest-type vegetation (Fig. 11b). Under the HadCM3 climate trajectory, ED2 and JULES project reductions in forest extent of 1.7% to 5.2% (Fig. 10b), with these losses occurring primarily in an arc extending from the northern portion of central Amazon to the eastern and southern Amazon (Fig. 11c). In the absence of CO₂ fertilization, the extent of the forest loss is more marked and extensive under the CCSM and HadCM3 trajectories (Fig. 11e and f).

Once the GOV scenario is superimposed on climate changes and rising CO₂, all simulations predict reductions in forest extent ranging from 6% to 21% (Fig. 10c). In the absence of CO₂ fertilization, the magnitude of the reduction of forest extent under the GOV scenario increases to 13–46% (Fig. 10c). Under the BAU land-use scenario, all simulations predict substantial reductions in forest extent with the reductions ranging from 37% to 61%, depending on the model, climate trajectory, and the presence or absence of CO₂ fertilization (Fig. 10d).

Discussion

Previous studies have analyzed the impacts of either changes in climate and CO₂ (e.g., Rammig *et al.*, 2010; Cox *et al.*, 2013; Huntingford *et al.*, 2013), or on the effects of fire (Aragão *et al.*, 2007) or land use (Soares-Filho *et al.*, 2012). In this analysis, we have used three terrestrial biosphere models to quantitatively assess the relative importance of these four different agents of ecosystem change for the fate of the Amazon region. To our knowledge, this is the first study to quantitatively assess the combined effects of these environmental drivers on the Amazon using a multimodel ensemble forced by multiple future climate change scenarios, multiple land-use scenarios, and incorporating the impacts of changing fire regimes. Below, we discuss the implications of our findings for our understanding of the expected fate of the Amazon forest over the coming century and their implications for future research priorities on this topic.

The relative importance of different drivers of ecosystem change

As can be seen in Fig. 4, all four of the environmental drivers considered in this study – climate, CO₂, land use, and fire – have significant impacts on Amazon aboveground biomass. Increasing CO₂ levels and business-as-usual (BAU) land transformation are, however, predicted to be largest drivers of Amazonian aboveground biomass (AGB) change over the 21st century (Figs 4–7).

In contrast to the consistently positive impacts of CO₂ and negative impacts of land use, the effects of changes in climate forcing on AGB are more variable, in both sign and magnitude. Under the more benign PCM and CCSM climate trajectories, the predicted impacts of climate change on Amazonian AGB range from modest increases in AGB (ED2 and IBIS) to modest losses (JULES) (Fig. 4), with the magnitude of these impacts being comparable to those of fire and GOV land use (Fig. 4). Under the more severe HadCM3 climate trajectory, the overall impact of climate change predicted by IBIS remains positive; however, in ED2 and JULES, the HadCM3 trajectory causes climate-driven losses of Amazonian AGB that exceed the losses arising from GOV land-use transformation.

Fire is also predicted to cause significant reductions Amazonian AGB (Fig. 4a–b), but its net effect is tempered by the more spatially localized nature of its impacts, which are largely confined to drier savanna regions and between the rainforest–savanna transition zones (Fig. 6b).

Overall simulations indicate that, regardless of the future climate scenario, the dynamics of land-use change in the region will remain a key determinant of Amazonian forest AGB (Fig. 7) and forest extent (Fig. 10). The model simulations predict shrinking of regional forest cover by 6–21% even under the GOV land-use scenario (Fig. 10c), implying that even under this conservative scenario, land-use impacts will exceed any potential forest cover expansion arising from either CO₂ fertilization or more favorable future climate. The BAU land-use scenario results in widespread AGB loss (Figure 6b), corresponding to 32–59 GtC over the 21st century, and reductions of Amazon forest extent by 37–48% (Fig. 10d). This highlights the catastrophic implications of unregulated anthropogenic activities in the Amazon. Recent evidence indicates that deforestation rates in the Brazilian Amazon have decreased markedly since 2004 due to better law enforcement and surveillance technology (INPE, 2014). If these new levels of enforcement are maintained, the BAU pattern of development will not occur. However, consideration of the BAU scenario alongside the GOV scenario emphasizes and quantifies the significance of continued law enforcement in maintaining the integrity of Amazon forest cover and carbon stocks.

Ecosystem responses to changes in climate forcing

The variation seen across the rows of Fig. 5 illustrates how uncertainties about the future climate forcing of the region remains an important source of variation in the future aboveground biomass of the Amazon. However, as the variation across the columns of Fig. 5 shows, the divergent predictions of the different terrestrial biosphere models under any given climate scenario are an equally large source of variation in future Amazon AGB patterns.

The standardized nature of the simulations conducted here shows that these differing macroscopic predictions reflect important differences in plant-level responses to changes in precipitation, temperature, and humidity within the three terrestrial biosphere models. With regard to the effects of increasing air temperature, the negative impacts of climate change on AGB in JULES (Fig. 5, bottom row) even in the most benign PCM projection, where water stress is projected to reduce in the future (Fig. 3a–b), indicates that increasing air temperatures negatively affect plant productivity in JULES compared to either ED2 or IBIS (Fig. 5). This accords the results of previous studies using MOSES-TRIFFID, the model from which JULES is derived, that also exhibits high sensitivities to rising air temperatures (Galbraith *et al.*, 2010; Huntingford *et al.*, 2013).

In addition to differential temperature sensitivities, the terrestrial biosphere models also exhibit markedly different levels of sensitivity to changes in water stress (Figs 8 and 9): ED2 has the highest sensitivity to water stress and extreme drought events, followed by JULES and then IBIS. These differing magnitudes of climate response predicted by the models align with the findings of the recent study by Powell *et al.* (2013), who evaluated the abilities of ED2, IBIS, JULES, and other several terrestrial biosphere models to capture the changes in AGB observed in two drought experiments that have been conducted in the Amazon (Nepstad *et al.*, 2007; Da Costa *et al.*, 2010). In the Powell *et al.* study, both JULES and IBIS predicted negligible reductions in aboveground biomass in response to the drought treatments. In contrast, ED2 captured the timing of the observed decline in AGB, although the magnitude of the predicted decline was greater than observed at one site and lower at the other. This suggests that, with respect to the expected impacts of increasing water stress on Amazonian AGB, the ecosystem's response is likely to be closer to ED2 predictions rather than those of IBIS or JULES. However, in flux tower model-data intercomparison studies, ED2 exhibited comparable skill to other models in capturing interannual variability in whole-ecosystem carbon fluxes (Von Randow *et al.*, 2013; Christoffersen *et al.*, 2014).

An important cause of ED2's higher sensitivity to water stress seen in Fig. 9a, and the Powell *et al.* (2013) analysis, is the dynamics of mortality within the model. As described in the *Materials and Methods* section, ED2 contains an explicit carbon balance-related per capita mortality term (sometimes referred to as a carbon starvation mortality term), while in IBIS and JULES, mortality is implicitly represented in terms of constant background rates of woody biomass turnover. Consequently, in ED2, changes in aboveground biomass can occur via impacts on rates of plant growth and via impacts on the rate of plant mortality.

More generally, the results shown in Figs 5, 8, and 9 highlight the urgent need for future Amazon ecosystem research to assess and improve the plant-level responses to climate variability and change within terrestrial biosphere models. How might this be achieved? The alignment between the predictions of the three models in this analysis and in Powell *et al.* (2013) study highlights the relevance and value of evaluating the ability of terrestrial biosphere models to predict the outcomes of manipulation experiments such as those of Nepstad *et al.* (2007) and Da Costa *et al.* (2010). The results in Fig. 8 suggest that another relevant metric for assessing the climate sensitivity of terrestrial biosphere models is their predicted patterns of interannual variability in AGB. Forest inventory measurements of AGB

dynamics, such as those available from the RAINFOR plot networks (Baker *et al.*, 2004; Malhi *et al.*, 2006; Phillips *et al.*, 2009) thus have the potential to act as valuable yardstick for assessing and constraining the climate sensitivities of terrestrial biosphere models and, by doing so, reduce the range of model outcomes seen across the columns of Fig. 5.

In addition to measurements of interannual variability in AGB and results of the drought manipulation experiments, a diverse array of other empirical studies relevant to determining climate sensitivity of Amazon forest forests have been conducted in recent years. In particular, flux tower measurements of seasonal variability in carbon and water fluxes (De Goncalves *et al.*, 2013; Von Randow *et al.*, 2013; Christoffersen *et al.*, 2014), leaf-to-canopy scale physiological studies (e.g., Doughty *et al.*, 2010), and studies across elevational gradients (e.g., Malhi *et al.*, 2010) have the potential to provide additional insights into the physiological mechanisms that underpin the climatological responses of Amazon forests.

CO₂ fertilization

All three terrestrial biosphere models predict a significant CO₂ fertilization effect on Amazonian AGB; however, there is a surprisingly large range in the predicted magnitude of the CO₂ fertilization impacts: ED2, IBIS, and JULES, respectively, predict AGB increases of 30–32%, 26–28%, and 5–8%, by the end of the century (Fig. 6a). This is surprising as all the models are using the widely utilized Farquhar–Leuning–Collatz photosynthesis model (Farquhar *et al.*, 1980; Collatz *et al.*, 1992; Leuning, 1995) and do not include any nutrient limitation effects on plant growth, which previous analyses (e.g., Thornton *et al.*, 2007) have shown, can strongly modulate the magnitude of CO₂ fertilization effects predicted by terrestrial biosphere models.

An important area for future modeling studies will be to understand the mechanistic underpinnings of the widely varying magnitude of CO₂ fertilization within the models. For example, to what extent is the weaker CO₂ fertilization in JULES compared to ED2 and IBIS linked to its high sensitivity to increasing air temperature? And what causes the divergence of the rates CO₂ fertilization seen in ED2 and IBIS trends after year 2060 (Fig. 8 panels d–f), given that their initial rates of enhancement are so similar?

At present, there is limited information available to assess the accuracy of the differing predictions seen in Fig. 6a. Analyses of forest inventory measurements across the basin indicate that AGB of Amazon forests has increased over recent decades, and it has been

suggested this may be attributable to rising CO₂ (Baker *et al.*, 2004; Phillips *et al.*, 2008). However, while free-air CO₂ enrichment (FACE) experiments in temperate forest ecosystems have found an average NPP increases of 23% in response to elevated CO₂ concentrations of 550 ppm (Norby *et al.*, 2005; and McCarthy *et al.* 2010), and evidence from chamber-based studies imply that CO₂-induced fertilization effects will occur in tropical forests (Lloyd & Farquhar, 2008), as yet, there have been no comparable FACE experiments conducted in tropical forests. The substantial differences in the species composition, climate, and soil nutrient availability in tropical and temperate forests may mean that the impacts of elevated CO₂ on tropical forest growth are considerably different than those measured in temperate zone studies. Hickler *et al.* (2008) argue that higher temperatures could result in higher CO₂ fertilization rates, while others argue that the CO₂ fertilization responses of tropical forest may be constrained by soil nutrient considerations, in particular low phosphorous availability (e.g., Reich *et al.*, 2009). Studies have also indicated that rising CO₂ levels favors the growth of lianas and fast-growing, but shorter-lived pioneer tree species (Phillips *et al.*, 2004; Schnitzer & Bongers, 2011), and it has been suggested that this may alter canopy composition and cause forest biomass to decline rather than increase (Körner, 2004). The recently funded Amazon FACE experiment (see Tollefsen, 2013) will provide much-needed experimental evidence regarding the nature and magnitude of CO₂ fertilization in Amazon forests, which promises to provide a much-needed empirical assessment of the magnitude of CO₂ fertilization predictions seen in Fig. 6a.

A second interesting result from that emerges from this analysis is prediction that elevated CO₂ will alleviate the negative impacts of water stress on the dynamics of aboveground biomass (Fig. 8, panels c and f), a finding that is consistent with results of Rammig *et al.* (2010) and Huntingford *et al.* (2013). FACE experiments in temperate grassland ecosystems (e.g., Field *et al.*, 1997) have shown that elevated CO₂ significantly increase water-use efficiency that can reduce levels of plant water stress. Chamber-based studies of tropical forest seedlings have also found water-use efficiency increases in response to elevated CO₂ (e.g., Oberbauer *et al.*, 1985); however, the applicability of these seedling-based studies to tropical forest canopies has been questioned (Körner, 1998). In addition to assessing the overall magnitude of CO₂-induced growth enhancement, another important priority for the Amazon FACE experiment will be to assess the predictions seen in Fig. 8 (panels c and f)

that elevated to CO₂ will mitigate the negative impacts of water stress arising from changes in precipitation across the region.

Fire dynamics

Our simulations also indicate that climate-induced changes in fire frequency and severity will also significantly impact Amazonian ecosystems, but the predicted magnitude and spatial extent of fire impacts varies considerably between the ED2 and IBIS model (Fig. 6b). The most notable differences occur in the savanna regions where IBIS predicts significant fire-driven losses of aboveground biomass while ED2 does not. In particular, this difference arises because of the interactive effect between climate and fire: In ED2, aboveground biomass and resulting fuel loads in these areas are low and are projected to remain low in the future, while climate change exerts a strong positive effect on AGB in IBIS in the savanna regions (Fig. 5) that increases fuel loads and correspondingly enhance fire occurrence and severity. Consequently, while ED2 and IBIS markedly differ in their predictions of the impacts of climate change (Fig. 5), their predictions for the net combined effect of these two drivers are quite similar (Fig. 9b).

The accuracies of terrestrial biosphere model predictions regarding how fire frequency and intensity will change over the coming century as a result of changes in climate forcing and climate- and CO₂-induced changes in ecosystem composition (Fig. 6b) are at present unknown. Terrestrial biosphere model evaluation exercises in the Amazon region have, thus far, focused on assessing model predictions of seasonal carbon and water fluxes (De Goncalves *et al.*, 2013; Von Randow *et al.*, 2013; Christoffersen *et al.*, 2014) and drought responses (Powell *et al.*, 2013) (though see Thonicke *et al.* (2010)). As results shown in Fig. 6b emphasize, however, there is an important need to evaluate terrestrial biosphere model predictions of fire dynamics for the Amazon and surrounding regions. Two relevant empirical metrics for these evaluations are satellite-derived information regarding the extant spatial patterns and interannual variability in the incidence and severity of fires in the region (e.g., Justice *et al.*, 2002; Chuvieco *et al.*, 2008; Van der Werf *et al.*, 2009) and the ability of the model to capture the outcome of fire experiments (e.g., Brando *et al.*, 2014).

Acknowledgements

This research was funded by a grant from the Andes-Amazon Initiative of The Gordon and Betty Moore Foundation. We thank the Land Surface Hydrology Group at Princeton University for

providing part of the bias-corrected PCM and NCEP climate data used in this study.

References

- Albani M, Medvigy D, Hurtt GC, Moorcroft PR (2006) The contributions of land-use change, CO₂ fertilization, and climate variability to the Eastern US carbon sink. *Global Change Biology*, **12**, 2370–2390.
- Aragão LEOC, Malhi Y, Roman-Cuesta RM, Saatchi S, Anderson LO, Shimabukuro YE (2007) Spatial patterns and fire response of recent Amazonian droughts. *Geophysical Research Letters*, **34**, L07701.
- Baccini A, Goetz SJ, Walker WS *et al.* (2012) Estimated carbon dioxide emissions from tropical deforestation improved by carbon-density maps. *Nature Climate Change*, **2**, 182–185.
- Baker TR, Phillips OL, Malhi Y *et al.* (2004) Increasing biomass in Amazonian forest plots. *Philosophical Transactions of the Royal Society of London Series B-Biological Sciences*, **359**, 353–365.
- Berg AA, Famiglietti JS, Walker JP, Houser PR (2003) Impact of bias correction to reanalysis products on simulations of North American soil moisture and hydrological fluxes. *Journal of Geophysical Research-Atmospheres*, **108**, 4490.
- Best MJ, Pryor M, Clark DB *et al.* (2011) The Joint UK Land Environment Simulator (JULES), model description - Part 1: energy and water fluxes. *Geoscientific Model Development*, **4**, 677–699.
- Betts RA, Cox PM, Collins M, Harris PP, Huntingford C, Jones CD (2004) The role of ecosystem-atmosphere interactions in simulated Amazonian precipitation decrease and forest dieback under global climate warming. *Theoretical and Applied Climatology*, **78**, 157–175.
- Brando PM, Goetz SJ, Baccini A, Nepstad DC, Beck PSA, Christman MC (2010) Seasonal and interannual variability of climate and vegetation indices across the Amazon. *Proceedings of the National Academy of Sciences of the United States of America*, **107**, 14685–14690.
- Brando PM, Balch JK, Nepstad DC *et al.* (2014) Abrupt increases in Amazonian tree mortality due to drought-fire interactions. *Proceedings of the National Academy of Sciences of the United States of America*, **111**, 6347–6352.
- Christoffersen BO, Restrepo-Coupe N, Arain MA *et al.* (2014) Mechanisms of water supply and vegetation demand govern the seasonality and magnitude of evapotranspiration in Amazonia and Cerrado. *Agricultural and Forest meteorology*, **191**, 33–50.
- Chuvieco E, Giglio L, Justice C (2008) Global characterization of fire activity: toward defining fire regimes from Earth observation data. *Global Change Biology*, **14**, 1488–1502.
- Clapp RB, Hornberger GM (1978) Empirical Equations for Some Soil Hydraulic Properties. *Water Resources Research*, **14**, 601–604.
- Clark DB, Mercado LM, Sitch S *et al.* (2011) The Joint UK Land Environment Simulator (JULES), model description - Part 2: carbon fluxes and vegetation dynamics. *Geoscientific Model Development*, **4**, 701–722.
- Cochrane MA (2003) Fire science for rainforests. *Nature*, **421**, 913–919.
- Collatz GJ, Ribas-Carbo M, Berry JA (1992) Coupled photosynthesis-stomatal conductance model for leaves of C4 plants. *Australian Journal of Plant Physiology*, **19**, 519–538.
- Costa MH, Pires GF (2010) Effects of Amazon and Central Brazil deforestation scenarios on the duration of the dry season in the arc of deforestation. *International Journal of Climatology*, **30**, 1970–1979.
- Cowling SA, Betts RA, Cox PM, Ettwein VJ, Jones CD, Maslin MA, Spall SA (2004) Contrasting simulated past and future responses of the Amazonian forest to atmospheric change. *Philosophical Transactions of the Royal Society B-Biological Sciences*, **359**, 539–547.
- Cox P (ed.) (2001) Description of the TRIFFID dynamic global vegetation model. In: *Hadley Centre Technical Note*. Hadley Centre, Met Office, Bracknell, UK.
- Cox PM, Betts RA, Bunton CB, Essery RLH, Rowntree PR, Smith J (1999) The impact of new land surface physics on the GCM simulation of climate and climate sensitivity. *Climate Dynamics*, **15**, 183–203.
- Cox PM, Betts RA, Collins M, Harris PP, Huntingford C, Jones CD (2004) Amazonian forest dieback under climate-carbon cycle projections for the 21st century. *Theoretical and Applied Climatology*, **78**, 137–156.
- Cox PM, Pearson D, Booth BB, Friedlingstein P, Huntingford C, Jones CD, Luke CM (2013) Sensitivity of tropical carbon to climate change constrained by carbon dioxide variability. *Nature*, **494**, 341–344.
- Da Costa ACL, Galbraith D, Almeida S *et al.* (2010) Effect of 7 yr of experimental drought on vegetation dynamics and biomass storage of an eastern Amazonian rainforest. *New Phytologist*, **187**, 579–591.

- De Gonalves LGG, Borak JS, Costa MH *et al.* (2013) Overview of the Large-Scale Biosphere-Atmosphere Experiment in Amazonia Data Model Intercomparison Project (LBA-DMIP). *Agricultural and Forest meteorology*, **182**, 111–127.
- De Mendonca MJC, Diaz MDV, Nepstad D, Da Motta RS, Alencar A, Gomes JC, Ortiz RA (2004) The economic cost of the use of fire in the Amazon. *Ecological Economics*, **49**, 89–105.
- Dimiceli CM, Carroll ML, Sohlberg RA, Huang C, Hansen MC, Townshend JRG (2011) *Vegetation Continuous Fields MOD44b*. University of Maryland, College Park, Maryland.
- Doughty CE, Flanner MG, Goulden ML (2010) Effect of smoke on subcanopy shaded light, canopy temperature, and carbon dioxide uptake in an Amazon rainforest. *Global Biogeochemical Cycles*, **24**, GB3015.
- Eltahir E, Bras RL (1993) On the response of the tropical atmosphere to large-scale deforestation. *Quarterly journal of the Royal Meteorological Society*, **119**, 779–793.
- Epica Community Members (2004) Eight glacial cycles from an Antarctic ice core. *Nature*, **429**, 623–628.
- Essery R, Clark DB (2003) Developments in the MOSES 2 land-surface model for PIL-PS 2e. *Global and Planetary Change*, **38**, 161–164.
- Farquhar GD, Caemmerer SV, Berry JA (1980) A biochemical-model of photosynthetic CO₂ assimilation in leaves of C-3 species. *Planta*, **149**, 78–90.
- Field CB, Lund CP, Chiariello NR, Mortimer BE (1997) CO₂ effects on the water budget of a grassland microcosm. *Global Change Biology*, **3**, 197–206.
- Foley JA, Prentice IC, Ramankutty N, Levis S, Pollard D, Sitch S, Haxeltine A (1996) An integrated biosphere model of land surface processes, terrestrial carbon balance, and vegetation dynamics. *Global Biogeochemical Cycles*, **10**, 603–628.
- Galbraith D, Levy PE, Sitch S, Huntingford C, Cox P, Williams M, Meir P (2010) Multiple mechanisms of Amazonian forest biomass losses in three dynamic global vegetation models under climate change. *New Phytologist*, **187**, 647–665.
- Golding N, Betts R (2008) Fire risk in Amazonia due to climate change in the HadCM3 climate model: potential interactions with deforestation. *Global Biogeochemical Cycles*, **22**, GB4007.
- Good P, Jones C, Lowe J, Betts R, Booth B, Huntingford C (2011) Quantifying environmental drivers of future tropical forest extent. *Journal of Climate*, **24**, 1337–1349.
- Goudriaan J (1977) *Crop Micrometeorology: a Simulation Study*. Centre for Agricultural Publication and Documentation, Wageningen, Netherlands.
- Hickler T, Smith B, Prentice IC, Mjofors K, Miller P, Arneth A, Sykes MT (2008) CO₂ fertilization in temperate FACE experiments not representative of boreal and tropical forests. *Global Change Biology*, **14**, 1531–1542.
- Hirota M, Holmgren M, Van Nes EH, Scheffer M (2011) Global resilience of Tropical Forest and Savanna to critical transitions. *Science*, **334**, 232–235.
- Houghton RA, Skole DL, Nobre CA, Hackler JL, Lawrence KT, Chomentowski WH (2000) Annual fluxes of carbon from deforestation and regrowth in the Brazilian Amazon. *Nature*, **403**, 301–304.
- Huntingford C, Zelazowski P, Galbraith D *et al.* (2013) Simulated resilience of tropical rainforests to CO₂-induced climate change. *Nature Geoscience*, **6**, 268–273.
- Hurt GC, Froliking S, Fearon MG *et al.* (2006) The underpinnings of land-use history: three centuries of global gridded land-use transitions, wood-harvest activity, and resulting secondary lands. *Global Change Biology*, **12**, 1208–1229.
- INPE (2014) Projeto PRODES: Monitoramento da Floresta Amazônica Brasileira por Satélite. Instituto Nacional de Pesquisas Espaciais, Brazil. São José dos Campos, Brazil.
- Justice CO, Giglio L, Korontzi S *et al.* (2002) The MODIS fire products. *Remote Sensing of Environment*, **83**, 244–262.
- Knox R (2012) *Land Conversion in Amazonia and Northern South America: Influences on Regional Hydrology and Ecosystem Response*. Unpublished Ph.D. Massachusetts Institute of Technology.
- Körner C (1998) Tropical forests in a CO₂-rich world. *Climatic Change*, **39**, 297–315.
- Körner C (2004) Through enhanced tree dynamics carbon dioxide enrichment may cause tropical forests to lose carbon. *Philosophical Transactions of the Royal Society of London Series B-Biological Sciences*, **359**, 493–498.
- Kucharik CJ, Foley JA, Delire C *et al.* (2000) Testing the performance of a Dynamic Global Ecosystem Model: water balance, carbon balance, and vegetation structure. *Global Biogeochemical Cycles*, **14**, 795–825.
- Lammering B, Dwyer I (2000) Improvement of water balance in land surface schemes by random cascade disaggregation of rainfall. *International Journal of Climatology*, **20**, 681–695.
- Le Quere C, Raupach MR, Canadell JG *et al.* (2009) Trends in the sources and sinks of carbon dioxide. *Nature Geoscience*, **2**, 831–836.
- Leuning R (1995) A critical-appraisal of a combined stomatal-photosynthesis model for C-3 plants. *Plant Cell and Environment*, **18**, 339–355.
- Lewis SL, Lopez-Gonzalez G, Sonke B *et al.* (2009) Increasing carbon storage in intact African tropical forests. *Nature*, **457**, 1003–1006.
- Lewis SL, Brando PM, Phillips OL, Van Der Heijden GMF, Nepstad D (2011) The 2010 Amazon drought. *Science*, **331**, 554.
- Li HB, Sheffield J, Wood EF (2010) Bias correction of monthly precipitation and temperature fields from Intergovernmental Panel on Climate Change AR4 models using equidistant quantile matching. *Journal of Geophysical Research-Atmospheres*, **115**, D10101.
- Lintner BR, Biasutti M, Diffenbaugh NS, Lee JE, Niznik MJ, Findell KL (2012) Amplification of wet and dry month occurrence over tropical land regions in response to global warming. *Journal of Geophysical Research-Atmospheres*, **117**, D11106, doi:10.1029/2012jd017499.
- Lloyd J, Farquhar GD (2008) Effects of rising temperatures and [CO₂] on the physiology of tropical forest trees. *Philosophical Transactions of the Royal Society B-Biological Sciences*, **363**, 1811–1817.
- Malhi Y, Wood D, Baker TR *et al.* (2006) The regional variation of aboveground live biomass in old-growth Amazonian forests. *Global Change Biology*, **12**, 1107–1138.
- Malhi Y, Roberts JT, Betts RA, Killeen TJ, Li WH, Nobre CA (2008) Climate change, deforestation, and the fate of the Amazon. *Science*, **319**, 169–172.
- Malhi Y, Aragao LEOC, Galbraith D *et al.* (2009) Exploring the likelihood and mechanism of a climate-change-induced dieback of the Amazon rainforest. *Proceedings of the National Academy of Sciences of the United States of America*, **106**, 20610–20615.
- Malhi Y, Silman MR, Salinas N, Bush M, Meir P, Saatchi S (2010) Elevation gradients in the tropics: laboratories for ecosystem ecology and global change research. *Global Change Biology*, **16**, 3171–3175.
- McCarthy HR, Oren R, Johnsen KH, *et al.* (2010) Re-assessment of plant carbon dynamics at the Duke free-air CO₂ enrichment site: interactions of atmospheric [CO₂] with nitrogen and water availability over stand development. *New Phytologist*, **185**, 514–528.
- Medvigy D, Wofsy SC, Munger JW, Hollinger DY, Moorcroft PR (2009) Mechanistic scaling of ecosystem function and dynamics in space and time: ecosystem Demography model version 2. *Journal of Geophysical Research-Biogeosciences*, **114**, G01002.
- Moorcroft PR, Hurtt GC, Pacala SW (2001) A method for scaling vegetation dynamics: the ecosystem demography model (ED). *Ecological Monographs*, **71**, 557–585.
- Nakicenovic N, Alcamo J, Davis G, Ai E (2000) *IPCC Special Report on Emissions Scenarios*. Cambridge University Press, Cambridge, UK & New York, NY, USA.
- Nepstad D, Lefebvre P, Da Silva UL *et al.* (2004) Amazon drought and its implications for forest flammability and tree growth: A basin-wide analysis. *Global Change Biology*, **10**, 704–717.
- Nepstad DC, Stickler CM, Almeida OT (2006) Globalization of the Amazon soy and beef industries: Opportunities for conservation. *Conservation Biology*, **20**, 1595–1603.
- Nepstad DC, Tohver IM, Ray D, Moutinho P, Cardinot G (2007) Mortality of large trees and lianas following experimental drought in an Amazon forest. *Ecology*, **88**, 2259–2269.
- Norby RJ, Delucia EH, Gielen B *et al.* (2005) Forest response to elevated CO₂ is conserved across a broad range of productivity. *Proceedings of the National Academy of Sciences*, **102**, 18052–18056.
- Oberbauer SF, Strain BR, Fetcher N (1985) Effect of CO₂ Enrichment on seedling physiology and growth of two tropical tree species. *Physiologia Plantarum*, **65**, 352–356.
- Phillips OL, Baker TR, Arroyo L *et al.* (2004) Pattern and process in Amazon tree turnover, 1976–2001. *Philosophical Transactions of the Royal Society of London Series B-Biological Sciences*, **359**, 381–407.
- Phillips OL, Lewis SL, Baker TR, Chao KJ, Higuchi N (2008) The changing Amazon forest. *Philosophical Transactions of the Royal Society B-Biological Sciences*, **363**, 1819–1827.
- Phillips OL, Aragao LEOC, Lewis SL *et al.* (2009) Drought sensitivity of the Amazon rainforest. *Science*, **323**, 1344–1347.
- Powell TL, Galbraith DR, Christoffersen BO *et al.* (2013) Confronting model predictions of carbon fluxes with measurements of Amazon forests subjected to experimental drought. *New Phytologist*, **200**, 350–364.
- Quesada CA, Lloyd J, Schwarz M *et al.* (2010) Variations in chemical and physical properties of Amazon forest soils in relation to their genesis. *Biogeosciences*, **7**, 1515–1541.
- Rammig A, Jupp T, Thonicke K *et al.* (2010) Estimating the risk of Amazonian forest dieback. *New Phytologist*, **187**, 694–706.
- Randall DA, Wood AW, Bony S *et al.* (2007) Climate models and their evaluation. In: *Climate Change 2007: The Physical Science Basis. Contribution of Working Group I to the*

- Fourth Assessment Report of the Intergovernmental Panel on Climate Change (eds Solomon S, Qin D, Manning M, Chen Z, Marquis M, Averyt KB, Tignor M, Miller HL), pp. 591–648. Cambridge University Press, New York.
- Reich PB, Oleksyn J, Wright IJ (2009) Leaf phosphorus influences the photosynthesis–nitrogen relation: a cross-biome analysis of 314 species. *Oecologia*, **160**, 207–212.
- Saatchi SS, Harris NL, Brown S *et al.* (2011) Benchmark map of forest carbon stocks in tropical regions across three continents. *Proceedings of the National Academy of Sciences of the United States of America*, **108**, 9899–9904.
- Saleska SR, Didan K, Huete AR, Da Rocha HR (2007) Amazon forests green-up during 2005 drought. *Science*, **318**, 612.
- Schnitzer SA, Bongers F (2011) Increasing liana abundance and biomass in tropical forests: emerging patterns and putative mechanisms. *Ecology Letters*, **14**, 397–406.
- Sheffield J, Goteti G, Wood EF (2006) Development of a 50-year high-resolution global dataset of meteorological forcings for land surface modeling. *Journal of Climate*, **19**, 3088–3111.
- Shuttleworth WJ (1993) Evaporation. In: *Handbook of Hydrology* (ed. Maidment DR), pp. 4.1–4.53. McGraw Hill, New York.
- Soares-Filho BS, Nepstad DC, Curran LM *et al.* (2006) Modelling conservation in the Amazon basin. *Nature*, **440**, 520–523.
- Soares-Filho BS, Lima L, Bowman M, Viana L, Gouveilo C (2012) *Challenges for a Low Carbon Agriculture and Forest Conservation in Brazil*. IADB, Washington, DC.
- Thonicke K, Spessa A, Prentice IC, Harrison SP, Dong L, Carmona-Moreno C (2010) The influence of vegetation, fire spread and fire behaviour on biomass burning and trace gas emissions: results from a process-based model. *Biogeosciences*, **7**, 1991–2011.
- Thornton PE, Lamarque JF, Rosenbloom NA, Mahowald NM (2007) Influence of carbon–nitrogen cycle coupling on land model response to CO₂ fertilization and climate variability. *Global Biogeochemical Cycles*, **21**, GB4018.
- Tollefsen J (2013) Experiment aims to steep rainforest in carbon dioxide. *Nature*, **496**, 405–406.
- Van der Werf GR, Morton DC, DeFries RS, Giglio L, Randerson JT, Collatz GJ, Kasibhatla PS (2009) Estimates of fire emissions from an active deforestation region in the southern Amazon based on satellite data and biogeochemical modeling. *Biogeosciences*, **6**, 235–249.
- Von Randow C, Zeri M, Restrepo-Coupe N *et al.* (2013) Inter-annual variability of carbon and water fluxes in Amazonian forest, Cerrado and pasture sites, as simulated by terrestrial biosphere models. *Agricultural and Forest meteorology*, **182**, 145–155.
- Zhang K, Kimball JS, Zhao M, Oechel WC, Cassano J, Running SW (2007) Sensitivity of pan-Arctic terrestrial net primary productivity simulations to daily surface meteorology from NCEP-NCAR and ERA-40 reanalysis. *Journal of Geophysical Research-Biogeoscience*, **112**, G01011.

Supporting Information

Additional Supporting Information may be found in the online version of this article:

Appendix S1. Projected climate change by the three GCMs.

Appendix S2. Spatial patterns of the Business-As-Usual and Governance land-use scenarios in Amazonia.

Appendix S3. Evaluation of the biosphere models' performance.

Appendix S4. Evaluation of association between water stress regime and AGB from model simulations and remote sensing estimates across the Amazon.

Figure S1. Maps of temporal trends from 2009 to 2100 in (a) annual air temperature, (b) vapor pressure deficit and (c) precipitation from the bias-corrected projections of three GCMs (i.e. PCM, CCSM3, and HadCM3); grey areas denote non-significant trends with 90% confidence.

Figure S2. Spatial patterns of land-use composition in 2100 under the (a) GOV and (b) BAU scenarios; the projected rates of land-use transformation were derived and extended from.

Figure S3. Spatial patterns of present-day (2000–2008) above-ground biomass across Amazonia from model estimates of (a) ED2, (b) IBIS, and (c) JULES, and remote sensing based estimates of (d) and (e), and (f) the quantile-quantile plots of model estimates against remote sensing (RS) based estimates.

Figure S4. Spatial patterns of present-day (2000–2008) percent tree cover across Amazonia from (a) ED2, (b) IBIS, (c) JULES, and (d) MODIS collection 5 MOD44B product. The inset graph shows the quantile-quantile plot of model estimates against remote sensing based estimates.

Table S1. Summary of the strength of association between water stress (MCWD) and AGB from model simulations and remote sensing estimates across the Amazon; the strength of association is quantified by Pearson's simply linear correlations and Kendall's Tau (i.e. the rank correlation).